Vol.68: e25240485, 2025
https://doi.org/10.1590/1678-4324-2025240485
ISSN 1678-4324 Online Edition

BABT
Brazilian Archives of Biology and Technology

Article - Biological, Medical and Health Technologies

The Glucagon-Like Peptide 1 Analog Liraglutide Impairs the Migration of Rat Intestinal Cells *in vitro*

Aline Gabriely Torres Duarte[1]
https://orcid.org/0009-0006-6186-164X

Jhony Willams Gusmão do Nascimento[2,3]
https://orcid.org/0000-0001-7244-8275

Everlaine Leite Estevam dos Santos Silva[1]
https://orcid.org/0009-0001-5530-6686

Luciana Aparecida Corá[2,3]
https://orcid.org/0000-0001-8242-3653

Maria Danielma dos Santos Reis[1,4*]
https://orcid.org/0000-0003-4119-4019

[1]Universidade Federal de Alagoas, Instituto de Ciências Biológicas e da Saúde, Laboratório de Biologia Celular, Alagoas, Brasil; [2]Universidade Estadual de Ciências da Saúde de Alagoas, Alagoas, Brasil; [3] Universidade Federal de Alagoas, Programa de Pós-Graduação em Biotecnologia, Rede Nordeste de Biotecnologia (RENORBIO), Alagoas, Brasil; [4]Instituto Nacional de Ciência e Tecnologia em Neuroimunomodulação (INCT-NIM), Rio de Janeiro, Brasil

Editor-in-Chief: Paulo Vitor Farago
Associate Editor: Jaiesa Zych Nadolny

Received: 05-Jun-2024; Accepted: 23-Jul-2025

*Correspondence: danielma.reis@icbs.ufal.br@e-mail.com; Tel.: +55-82-987630201 (M.D.S.R.).

HIGHLIGHTS

- Liraglutide is a GLP-1 analog for treatment of diabetes and obesity.
- In vitro treatment with liraglutide prevented rat intestinal cells apoptosis.
- Migration of intestinal cells was impaired during exposure to liraglutide in vitro.

Abstract: Liraglutide plays a crucial role in managing weight and regulating glucose levels, but it can have adverse effects, particularly on the gastrointestinal tract. Here, we assessed the impact of liraglutide on the viability, cell death, morphology, reorganization of the actin cytoskeleton, and migration of rat intestinal epithelial cells. There was no change in the viability of cells treated with liraglutide at concentrations of 0.25, 0.5, and 1 μM, however, high concentrations of the drug reduced IEC- 6 cell viability. Additionally, the treatment with low doses of liraglutide decreased the rate of apoptosis of IEC-6 cells relative to the control. Also, the treated cells showed a modified actin cytoskeleton, with prominent stress fibers. Regarding cell migration, there was a decrease in the percentage of closure of the cell-free area over 24 h, relative to the untreated cells. This study revealed the direct effects of liraglutide on intestinal cells, including reduced apoptosis rates, actin cytoskeleton alterations, and inhibited cell migration.

Keywords: Glucagon-like peptide 1 analogs; liraglutide, cell viability; cell migration.

GRAPHICAL ABSTRACT

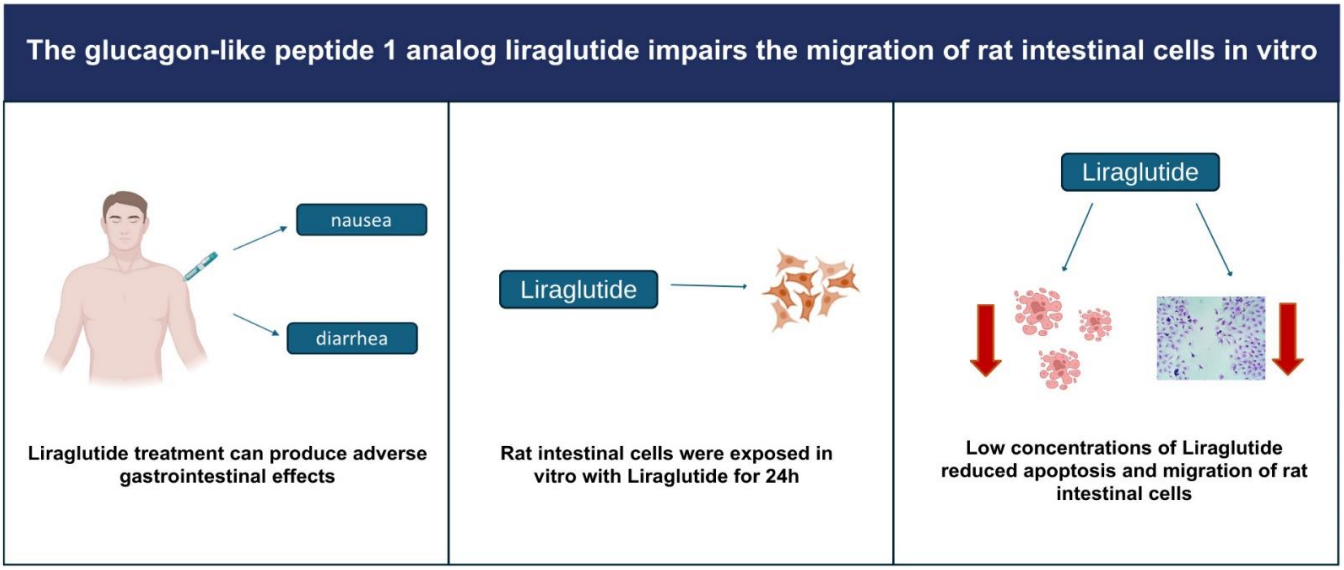

INTRODUCTION

Food intake triggers several physiological responses in the digestive system, including the release of gastrointestinal hormones from enteroendocrine cells that are involved in appetite regulation [1], the main ones are the incretins, glucose-dependent insulinotropic polypeptide and glucagon-like peptide 1 (GLP-1). The expression of GLP-1 receptors (GLP-1R) occurs in neurons of the myenteric plexus [2, 3] and, through them, GLP-1 acts on the physiological regulation of the gastrointestinal tract [4]. The secretion of GLP-1 provides adequate release of insulin by the endocrine pancreas, in addition to delaying the entry of chyme into the intestine through the decrease of gastric motility and acid secretion [5]. Therefore, factors that interfere with the regulation of the release of these hormones affect energy homeostasis and contribute to obesity, a chronic disease that presents clinical complications associated with multiple metabolic disorders. In this context, drugs that target GLP-1 activation pathways are promising for treating obesity [6].

Liraglutide is a long-acting GLP-1 analog that was initially made available for treating type 2 diabetes. However, due to its ability to induce weight loss, liraglutide has become the drug of choice for treating obesity, associated with diet and exercise [7, 8]. This drug has 97% sequence homology with human GLP-1 and binds to and activates GLP-1R, thus potentiating glucose-dependent insulin secretion by β-pancreatic cells. Studies in animal models have shown that liraglutide increases satiety, stimulates insulin secretion, slows gastric emptying, and inhibits duodenal motility [9].

In addition to the known actions of GLP-1 on gastrointestinal motility and insulin secretion, liraglutide acts as a protective factor of intestinal barrier integrity as it has a positive effect on mucus secretion, decreasing inflammation, and protecting the intestinal mucosa [10]. Also, some studies demonstrated that this peptide may regulate the gut microbiota, impacting insulin secretion and the regulation of the intestinal immune system [11, 12]. However, concentration-dependent cytotoxic effects of these analogs have been reported [10], such as inhibition of cell growth [3], in addition to gastrointestinal adverse effects as nausea, vomiting, diarrhea, and constipation [13].

In the light of the widespread and indiscriminate use of GLP-1 analogs for weight loss, it is important to conduct research to elucidate the effects of these drugs in the organism, particularly in intestinal cells. In this context, our previous study demonstrated that high doses of liraglutide improved obesity-related parameters and reduced inflammation in intestinal tissue [14]. However, the direct effect on intestinal cells still requires further investigation. Therefore, this study aimed to investigate the specific impacts of the GLP-1 analog liraglutide on intestinal epithelial cells.

MATERIAL AND METHODS

Cell culture

Rat intestinal epithelial cells of the IEC-6 cell line (Rio de Janeiro cell bank; BCRJ) were cultured in Dulbecco's Modified Eagle's Medium (DMEM, Sigma-Aldrich) with high glucose concentration (4.5 g/L) and supplemented with 10% fetal bovine serum (FBS), 4 mM of L-glutamine, 0.1 U/mL of human insulin (Invitrogen), and 0.02 ml of penicillin/streptomycin solution. When necessary, the passage of cells was performed using 0.25% trypsin-EDTA solution. They were incubated at 37°C with 5% CO2 until being used in the experimental procedures.

Cell viability

The cells were seeded at a concentration of 10^4 cells/well in a 96-well plate. The treatment was performed on the following day using liraglutide hydrochloride (Victoza®, Novo Nordisk) at concentrations of 0.25, 0.5, 1, 25, 50, and 100 µM, diluted in DMEM medium with 2% SBF for 24 h. After the treatment, the cells were incubated with thiazolyl blue tetrazolium bromide (MTT; 5 mg/mL) for 3 h. After this period, the medium was removed and dimethylsulfoxide (DMSO) was added for cell lysis and release of formazan crystals. MTT absorbance was measured by spectrophotometry (Polaris^2 Celer Biotecnologia S.A) at a wavelength of 540 nm.

Quantification of apoptosis and necrosis

Cell apoptosis was determined by examining cell morphology and DNA degradation using acridine orange (AO, 1 mg/mL) and propidium iodide (PI, 1 mg/mL) under a fluorescence microscope. The cells were seeded at a concentration of 10^4 cells/well in 24-well plates containing round coverslips and treated with liraglutide at concentrations of 0.25, 0.5, and 1 µM diluted in DMEM 2% SBF for 24 h. For labeling, AO and PI were diluted in 1X PBS. After treatment, the cells were washed with PBS and incubated for 2 min with the solution containing the dyes. After this period, the coverslips were mounted on glass slides and visualized under a Nikon Eclipse 50i fluorescence microscope. AO labeling was visualized using a 528-nm filter. To visualize the cells labeled with PI, a 461-nm filter was used. The analysis of cell apoptosis was based on cell staining and morphology [15], divided into three groups: viable cells – with the nucleus stained in green (Figure 1 a); cells in apoptosis – stained in green (Figure 1 b), with changes in their membrane; cells in necrosis – stained in orange or red (Figure 1 c). The cells were counted in five random fields of each well using the ImageJ software. The frequency of viable, apoptotic, and necrotic cells was calculated according to the equation:

$$\%=a/t \times 100$$

where: a= number of viable /apoptotic /necrotic cells in the field; t = total number of cells per field.

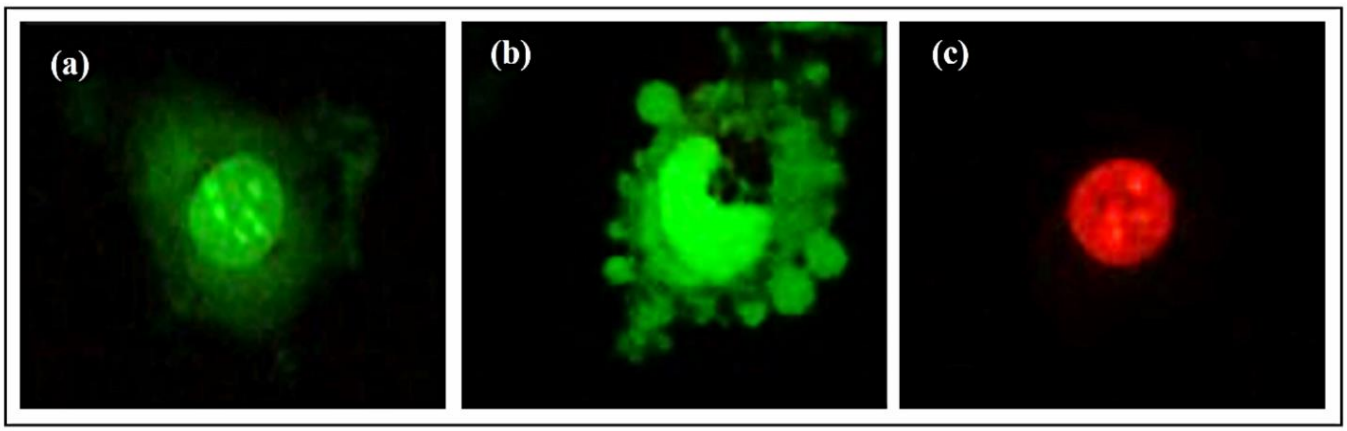

Figure 1. Examples of the morphological aspects of IEC-6 after acridine orange (green) and propidium iodide (red) staining for cell death evaluatuion. (a) viable cells; (b) apoptotic cells; (c) necrotic cells. Photomicrographs were obtained from IEC-6 cultures at 200X magnification and zoom in pictures were obtained to show different cell morphologies.

Morphological analysis

For the morphological analysis and evaluation of the F-actin cytoskeleton, IEC-6 cells were seeded at a concentration of 5×10^3 cells/well in Labtek-type 8-well plates. After 24 h, the cells were treated with liraglutide diluted in DMEM 2% FBS at concentrations of 0.25, 0.5, and 1 µM for a period of 24 h. Then, the cells were washed with 1X PBS and fixed with 4% paraformaldehyde for 10 min. After fixation, the cells were washed again with 1X PBS and permeabilized with Triton X-100 at 0.5%. After washing with 1X PBS, the cells were labeled for F-actin with phalloidin conjugated with fluorescein isothiocyanate (FITC) for a period of 1 h in the dark. In the final step, after another PBS wash, the slides were mounted with glycerol at a ratio of 1:3 in PBS for analysis under the Nikon Eclipse 50i fluorescence microscope. Labeling analysis was performed qualitatively, observing the morphological changes and the arrangement of the F-actin filaments.

Cell migration

The scratch wound-healing assay was used to quantify the percentage of migration of IEC-6 cells. The cells were seeded at a concentration of 8×10^4 cells/well in a 24-well plate. On the day of treatment, a cell-free area was made on the monolayer of cells using a sterile tip. Then, the cells were washed with PBS to remove cellular debris and treated with liraglutide hydrochloride at concentrations of 0.25, 0.5, and 1 µM diluted in DMEM 2% FBS. Cell migration was followed using an inverted light microscope (T1-SM Nikon) until the closure of the cell-free area, with photomicrographs taken at 0, 6, 12, and 24 h. After 24 h, the cells were fixed with 4% paraformaldehyde for 10 min, washed with PBS 1X, and stained with crystal violet (2 mg/mL) for 5 min. The cells were visualized under an inverted microscope and photomicrographs were taken using the 20X objective. The quantification of the area of cell migration was performed using the ImageJ software, in which the area (in μm^2/pixel) that remained open after the treatment period was manually delimited. The calculation of the percentage of closure of the cell-free area was performed according to the following equation:

$$\%\ of\ closure = (at0 - ath/\ at0) \times 100$$

Where: At0 is the scratched area at time zero and Ath is the scratched area at the time of analysis.

Statistical analysis

Statistical analysis was performed using the GraphPad Prism software, version 7.00 (GraphPad Prism Software, Inc.). The data obtained were evaluated by ANOVA followed by Tukey's post-test, with a significance level set at $p < 0.05$ and were expressed as mean ± standard error of the mean (SEM).

RESULTS

Effect of liraglutide on intestinal cell viability

It was found that after 24 h of treatment with liraglutide at concentrations of 25, 50, and 100 µM there was a significant reduction of approximately 25% and 30% in cell viability compared to the group of untreated cells (control). In contrast, concentrations of 0.25, 0.5, and 1 µM did not significantly alter cell viability (Figure 2).

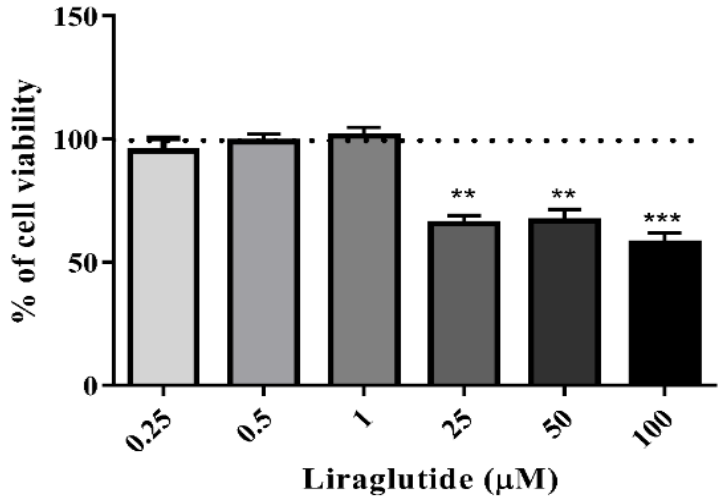

Figure 2. The percentage of viability of IEC-6 cells after treatment with liraglutide at concentrations of 0.25, 0.5, 1, 25, 50, and 100 µM for 24 h. The viability of the untreated cells was considered as 100%. **p < 0.01 and ***p < 0.0001 relative to the control.

Evaluation of apoptosis and cellular necrosis

It was observed that treatment with liraglutide significantly decreased the percentage of apoptotic cells (2.5% at 0.25 μM; 1.62% at 0.5 μM; and 1.66% at 1 μM) relative to the control (9%) (Figures 3 and 4). However, there was no difference in the percentage of viable and necrotic cells (Figure 4).

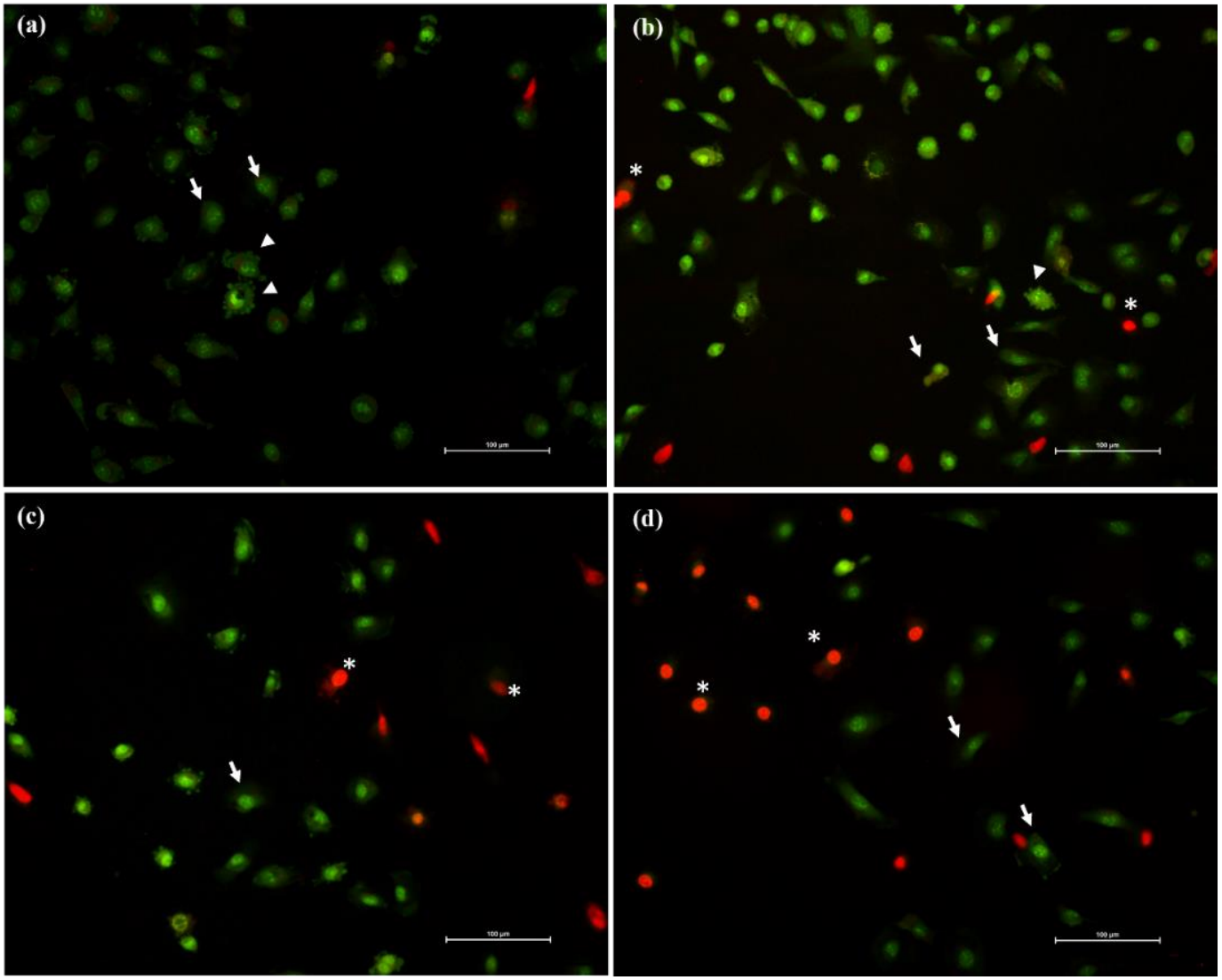

Figure 3. The effect of liraglutide on apoptosis and necrosis of rat intestinal epithelial cells after 24 h. The photomicrographs shown in (a) cells of the control group; (b) cells treated with liraglutide at a concentration of 0.25 μM; (c) cells treated with liraglutide at a concentration of 0.5 μM and (d) cells treated with liraglutide at a concentration of 1 μM after staining with acridine orange (green) and propidium iodide (red). The arrowheads indicate cells in apoptosis, with blistering on the membrane; the asterisks indicate cells in necrosis, and the white arrows indicate viable cells. The magnification of 200X. Size bar= 100 μm.

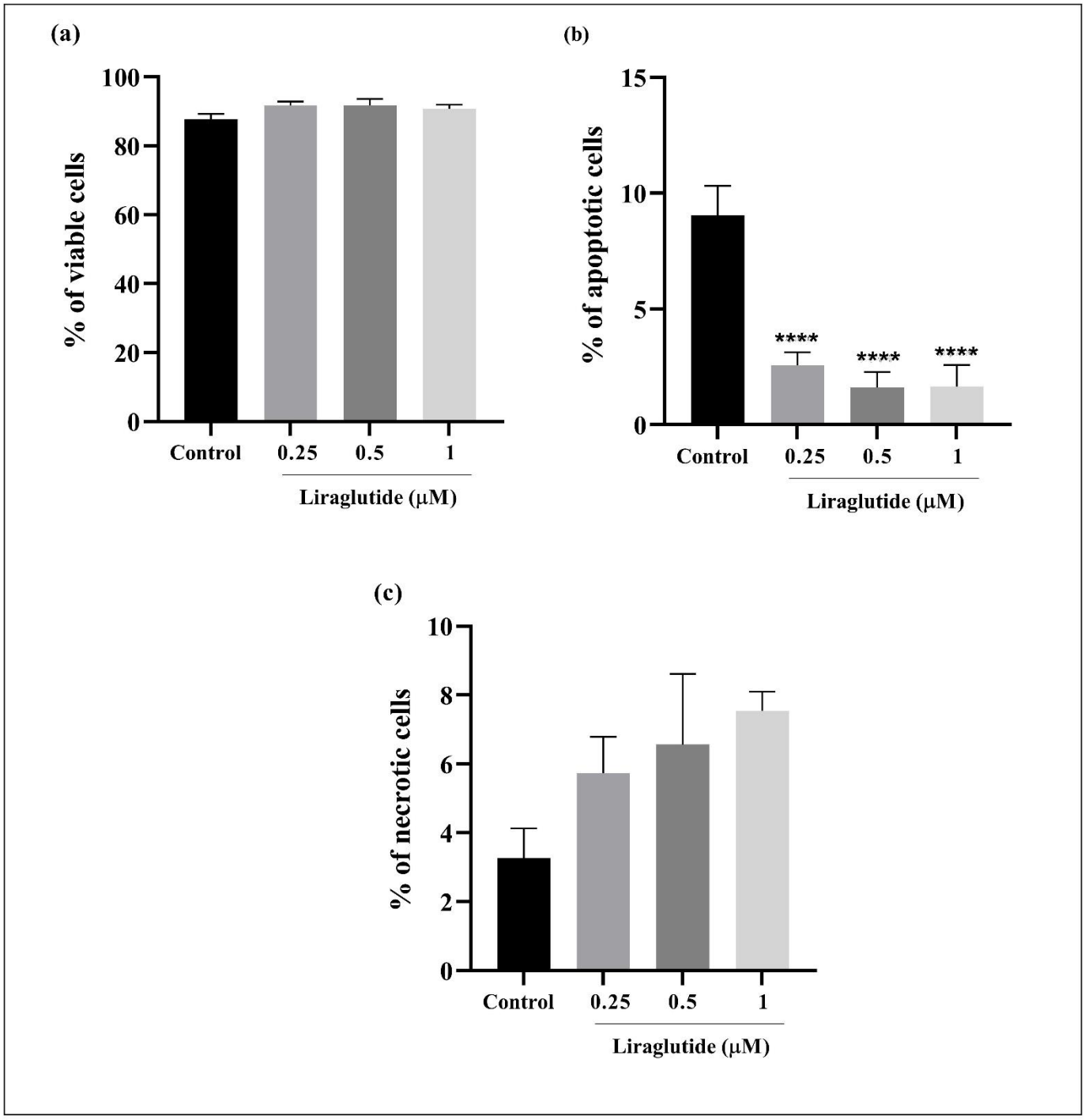

Figure 4. Percentage of viable (a), apoptotic (b), and necrotic (c) cells after treatment with liraglutide at concentrations of 0.25, 0.5, and 1.0 μM. The bars indicate mean ± SEM. ****$p < 0.0001$ relative to the control.

Effect of liraglutide on the morphology and actin cytoskeleton of IEC-6 cells

Figure 5 shows the morphological changes exhibited by IEC-6 cells after treatment with liraglutide. The untreated IEC-6 cells exhibited typical epithelial morphology, i.e., a monolayer of cells with polygonal shape (Figure 5a). After treatment with the drug at concentrations of 0.25 μM (Figure 5b), 0.5 μM (Figure 5c), and 1.0 μM (Figure 5d), the cells showed reduced size and less cell-to-cell contact, suggesting an effect on cell junctions. Regarding the organization of the actin cytoskeleton in IEC-6 cells, in the untreated cells there were F-actin filaments, forming fibers in the cell periphery, mainly in the regions of cell–cell junctions, as shown by the increased fluorescence intensity at the site (Figure 5a). The cells treated with liraglutide at concentrations of 0.25 (Figure 5b), 0.5 (Figure 5c), and 1 μM (Figure 5d) had prominent stress fibers, with distinct rearrangements, which were concentrated both inside and in the periphery of cells, in perpendicular bundles.

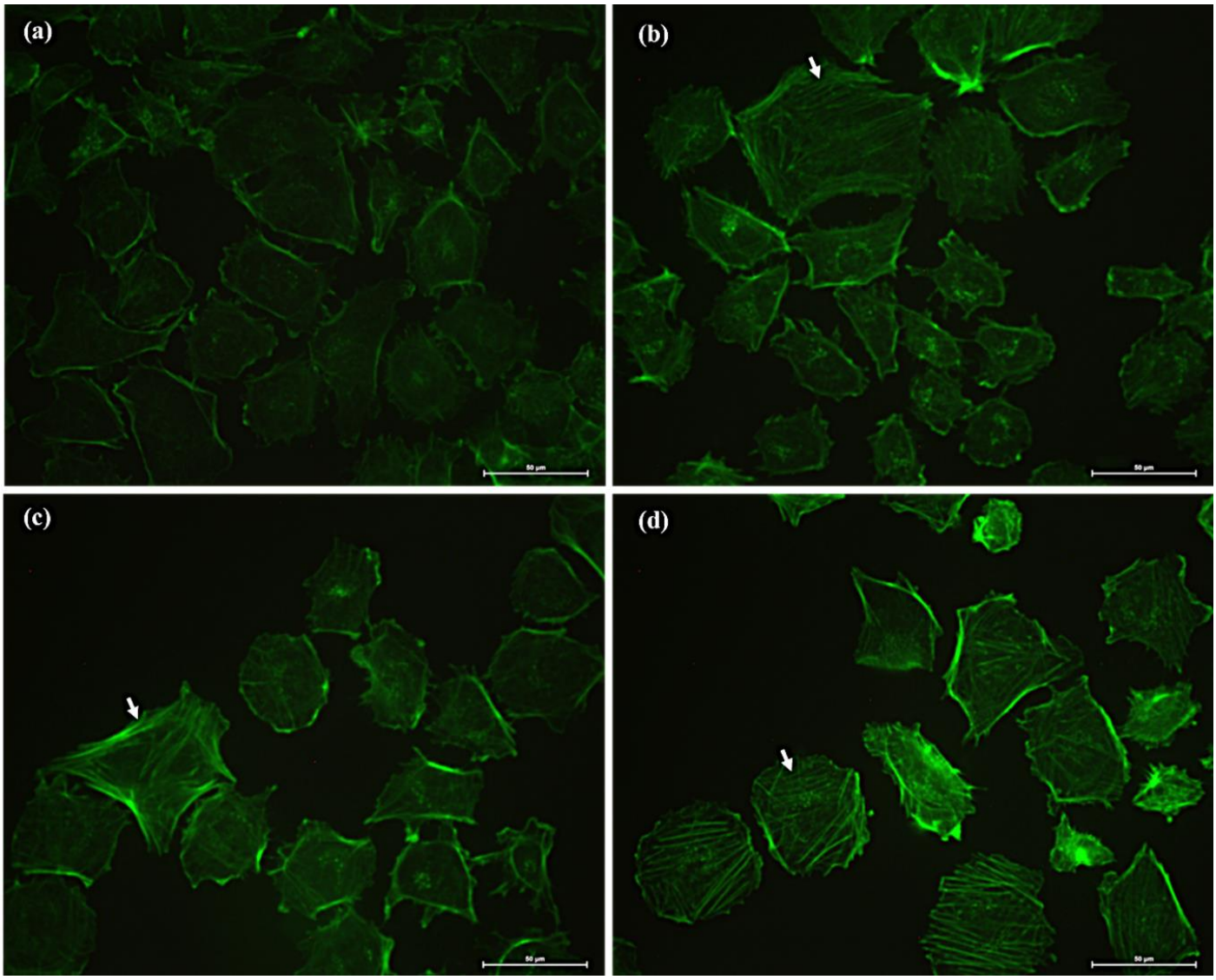

Figure 5. The effect of liraglutide on the morphology and F-actin cytoskeleton in the IEC-6 cells. The photomicrographs shown in (a) cells of the control group; (b) cells treated with liraglutide at 0.25 µM; (c) cells treated with liraglutide at 0.5 µM and (d) cells treated with liraglutide at 1 µM after labeling of actin filaments with phalloidin-FITC (green). The white arrows indicate the stress fibers. The magnification of 400X. Size bar= 50 µm.

Evaluation of cell migration during treatment with liraglutide

Figure 6 illustrates the effect of different concentrations of liraglutide on cell migration before (t = 0 h), 6 and 12 h after treatment. The cells treated with liraglutide showed a lower closure rate than the control. Figure 7 shows the cells of the control group occupying the entire area injured after 24 h of treatment, whereas cell-free areas are still observed in the treated groups. There was a significant difference in the percentage of closure between the untreated and treated cells at 1 µM of liraglutide at 6 h, and 0.25, 0.5 and 1 µM over 12 h and 24 h of treatment, respectively (Figure 8).

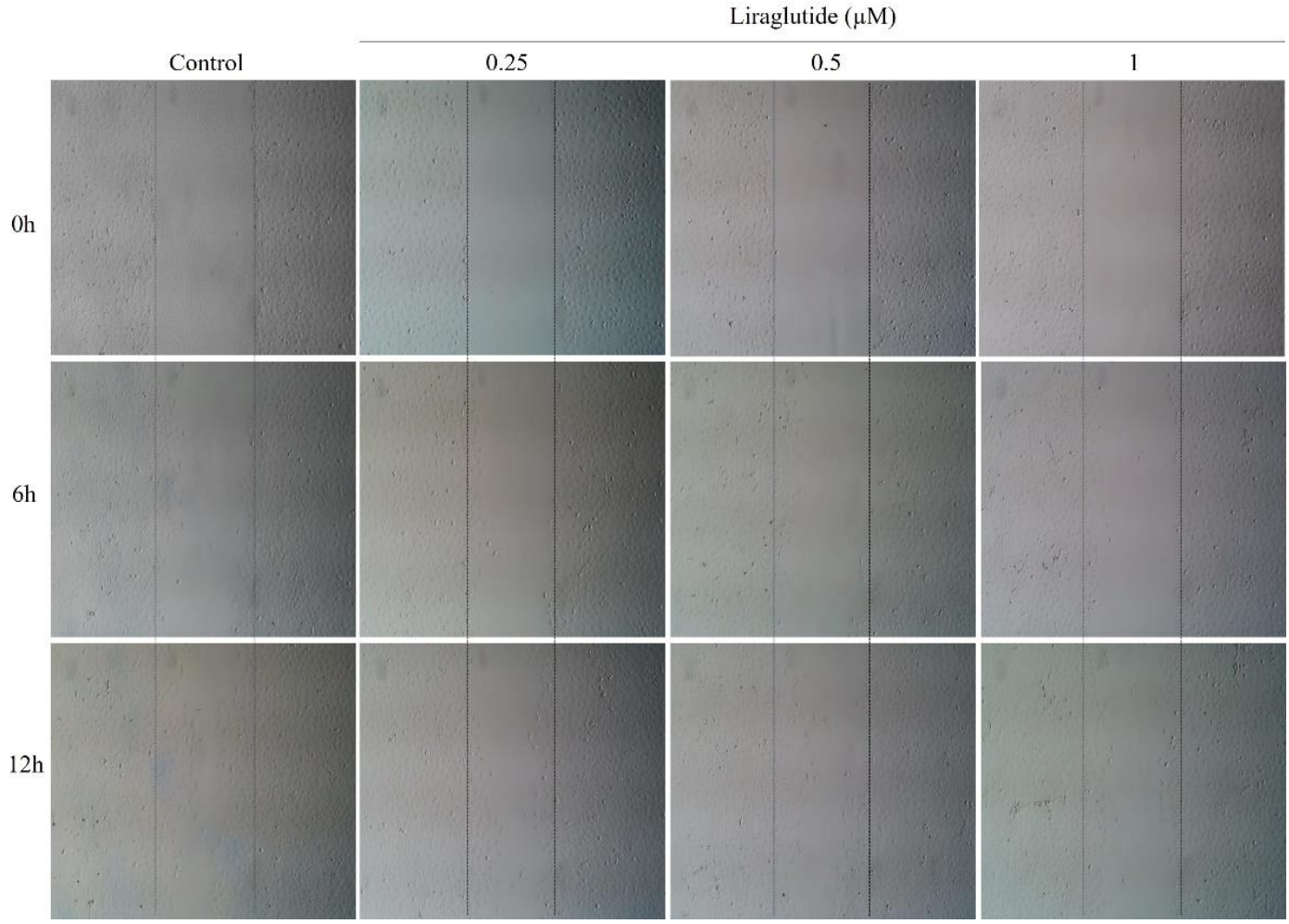

Figure 6. The effect of liraglutide treatment at concentrations of 0.25, 0.5, and 1 μM on IEC-6 cell migration. Cell migration was followed under the inverted light microscope until the closure of the cell-free area at intervals of 0, 6, and 12 h after treatment. Dotted lines delimit de cell-free area in th e 0h. The magnification of 40X.

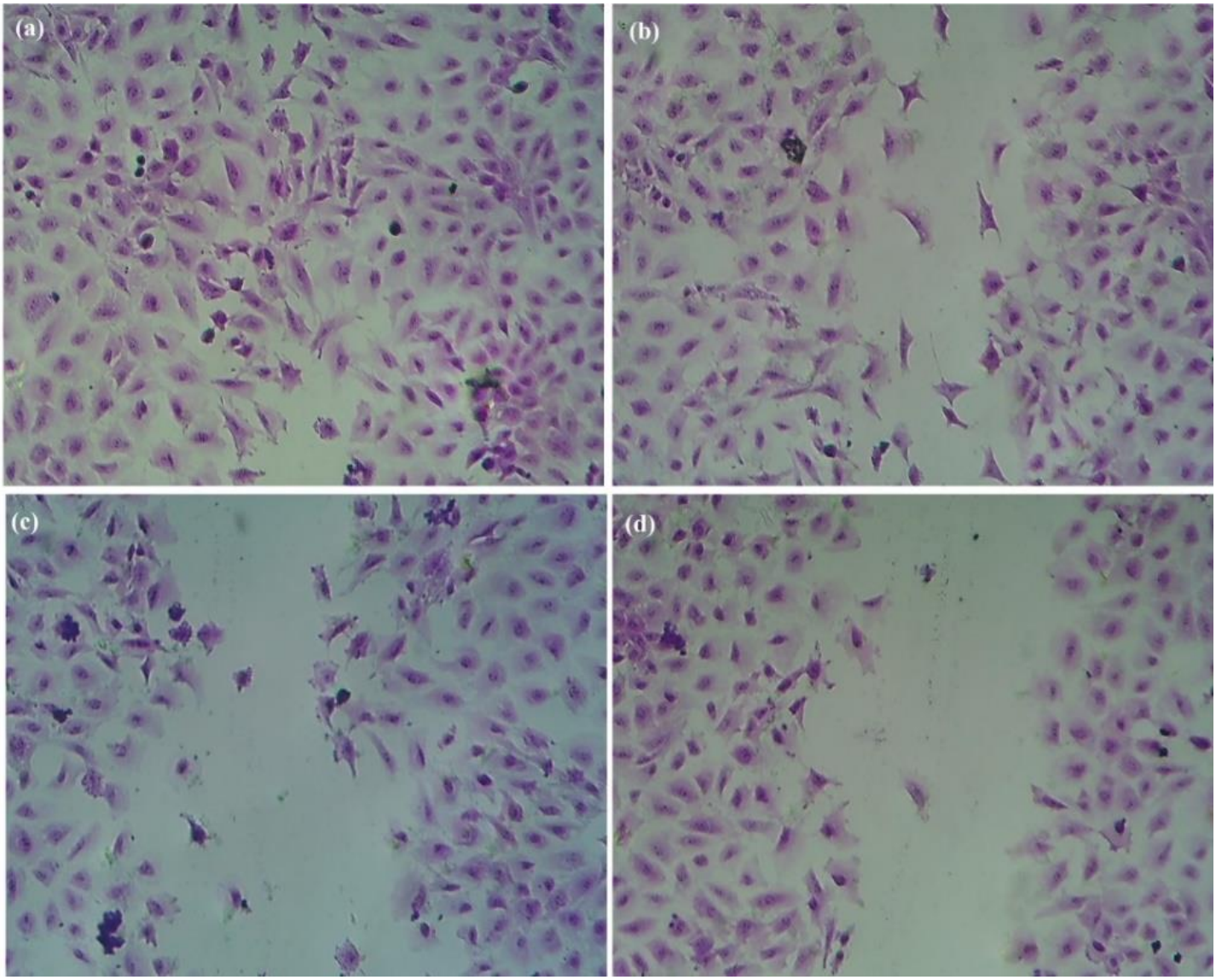

Figure 7. The effect of liraglutide on the migration of IEC-6 cells after 24 h of treatment. In (a) cells of the control group; (b) cells treated with liraglutide at a concentration of 0.25 µM; (c) cells treated with liraglutide at a concentration of 0.5 µM and (d) cells treated with liraglutide at a concentration of 1 µM. Staining with 2% crystal violet. The magnification of 200X.

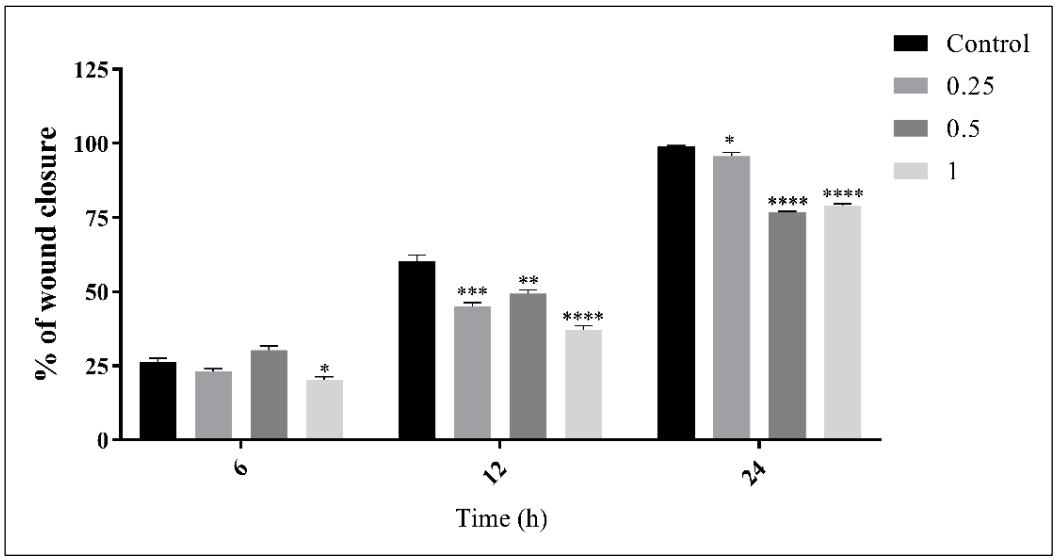

Figure 8. The percentage of migration of IEC-6 cells treated with liraglutide. The graph shows the percentage of the closure of the cell-free area over time. The data are expressed as mean ± SEM. *p < 0.05, ** and ***p < 0.01, **** p<0.0001 compared to the control.

DISCUSSION

This study showed that treatment with liraglutide affected the viability, arrangement of the F-actin cytoskeleton, and migration of IEC-6 intestinal epithelial cells. The higher concentrations were responsible for the reduction of approximately 25% and 30% in cell viability, while concentrations of 0.25, 0.5, and 1 μM did not significantly alter cell viability. Similarly, a study by Takizawa and coauthors (2022) [3] showed that IEC-6 cell growth was slightly concentration-dependently inhibited by liraglutide. This finding may be related to the appearance of more pronounced gastrointestinal effects at the beginning of treatment and when the weekly dose is changed for treating obesity [16]

Moreover, it was observed that treatment with liraglutide reduced the number of apoptotic cells. This finding is in line with previous studies on the role of GLP-1 in cellular apoptosis. Hui and coauthors (2003) [17] found that GLP-1 inhibited apoptosis in mouse insulinoma (MIN6) cells through a signaling pathway dependent on cyclic adenosine monophosphate (cAMP) and phosphoinositide 3-kinase (PI3K). Additionally, research with freshly isolated human pancreatic islets showed that treatment with GLP-1 reduced the number of apoptotic cells through the downregulation of active caspase-3 and the upregulation of the anti-apoptotic protein BCL-2 [18]. Similarly, a study by Challa and coauthors (2012) [19] showed a decrease in apoptosis in pre-adipocytes of the 3T3-L1 fibroblast treated with GLP-1 and liraglutide at a concentration of 0.01 μM. The authors showed that the protective effect of the substances was a result of the activation of signal-regulated extracellular kinase (ERK), protein kinase C (PKC), and serine/threonine kinase (AKT) signaling pathways, which are important in the suppression of apoptosis. According to Quoyer and coauthors (2010) [20], the inhibition of apoptosis in pancreatic β cells by GLP-1 is mediated by β-arrestin 1, causing the activation of the ERK1/2 pathway. That study demonstrated that the activation of this pathway leads to the phosphorylation of the homologous Bcl-xL/Bcl-2-associated death promoter (BAD), thereby inactivating it. Similarly, Yao and coauthors (2021) [21] showed the protective capacity of liraglutide against apoptosis of nucleus pulposus cells, causing decreased expression of pro-apoptosis molecules, such as BCL2-associated protein X, cell death (BAX), and caspase-3 regulator and increased BCL2 protein. It was found that exenatide inhibited the apoptosis of baby hamster kidney fibroblasts through the same antiapoptotic mechanism, reducing the synthesis of caspase-3, caspase-8, and caspase-9 [22]. Therefore, we can argue that GLP-1 and liraglutide prevent the apoptosis of IEC-6 cells by regulating the classic cell death signaling pathway.

Studies have shown that the permeability of intercellular connections can be altered because of contact with toxic inputs and pathological agents [23, 24, 25, 26]. This may occur due to a change in the arrangement of the F-actin filaments that make up the enterocyte membrane, causing pores to open at the adherent junctions and leading to increased intestinal absorption [23, 25]. It was observed that the liraglutide-treated cells showed cytoskeletal reorganization and prominent stress fibers compared with the untreated cells. Similar results were reported by Zhao et al. (2019) [27], who showed that treatment with exenatide, a GLP-1 analog, led to increased stress fibers and morphological changes in SH-SY5Y human neuroblastoma cell lines and in rat pheochromocytoma-derived PC12 cells. The remodeling of the cytoskeleton can be triggered by the phosphorylation of the enzyme cofilin, which is responsible for the state of polymerization and depolymerization of actin fibers. Based on this, it was found that cells treated with exenatide showed an increase in the expression of phosphorylated cofilin (inactivation), which may be an indicative of actin polymerization [27]. This reorganization of the cytoskeleton may be associated with a decrease in the migratory capacity of the cells, as will be discussed below.

As presented in the results, liraglutide significantly decreased the ability of intestinal epithelial cells of rats to migrate during the 24-h treatment. Similarly, treatment with exenatide significantly reduced the migration of SH-SY5Y cells through the inactivation of cofilin [2]. In this context, the reorganization of actin fibers may be an important factor for cell motility. The ribosomal protein S6 kinase β-1 (p70 S6K) is important for the organization of actin fibers and regulation of cell migration. According to Berven et al. (2004) [28], p70 S6K can be found in the actin arc, where the activators of cell motility are, and in the stress fibers that inhibit the migration process. Factors such as rapamycin may inhibit the migration of fibroblasts and epithelial cells through the inhibition of p70 S6K [29]. Thus, it is possible to suggest that the decrease in cell migration induced by GLP-1 analogs is mediated by the inactivation of proteins related to the reorganization of the actin cytoskeleton.

CONCLUSION

In summary, the findings of this study show that liraglutide directly affects the intestinal epithelial cells, thereby influencing cell death processes and the arrangement of the F-actin cytoskeleton. Importantly, this drug has a negative effect on the migration of intestinal epithelial cells. However, future studies are needed to relate these actions and their mechanisms to gastrointestinal clinical outcomes.

Funding: This research was funded by by the Dean of Research and Postgraduate Studies at Alagoas State University of Health Sciences (BIPES Research Fellowship 2021/2022).
Acknowledgments: The authors would like to thank Enago (www.enago.com) for the English language review.
Conflicts of Interest: The authors declare no conflict of interest.

Data Availability Statement: Research data are only available upon request for corresponding author.

REFERENCES

1. Miron I, Dumitrascu DL. Gastrointestinal motility disorders in obesity. Acta Endocrinol. (Buchar.) [Internet]. 2019;15(4):497–504. Available from: http://dx.doi.org/10.4183/aeb.2019.497
2. Körner M, Stöckli M, Waser B, Reubi JC. GLP-1 receptor expression in human tumors and human normal tissues: potential for in vivo targeting. J. Nucl. Med. [Internet]. 2007;48(5):736–43. Available from: http://dx.doi.org/10.2967/jnumed.106.038679
3. Takizawa Y, Oguri J, Uno M, Onsui A, Ishimura A, Kurita T, et al. Effects of A GLP-1 receptor agonist on gastrointestinal epithelial cells. Sch. Acad. J. Pharm. [Internet]. 2022;11(4):60–6. Available from: http://dx.doi.org/10.36347/sajp.2022.v11i04.002
4. Nauck MA, Niedereichholz U, Ettler R, Holst JJ, Ørskov C, Ritzel R, et al. Glucagon-like peptide 1 inhibition of gastric emptying outweighs its insulinotropic effects in healthy humans. Am. J. Physiol. Endocrinol. Metab. [Internet]. 1997;273(5):E981–8. Available from: http://dx.doi.org/10.1152/ajpendo.1997.273.5.E981
5. Maselli DB, Camilleri M. Effects of GLP-1 and its analogs on gastric physiology in diabetes mellitus and obesity. Adv. Exp. Med. Biol. [Internet]. 2021;1307:171–92. Available from: http://dx.doi.org/10.1007/5584_2020_496
6. Knudsen LB, Lau J. The discovery and development of liraglutide and semaglutide. Front. Endocrinol. (Lausanne) [Internet]. 2019;10:155. Available from: http://dx.doi.org/10.3389/fendo.2019.00155
7. Ladenheim EE. Liraglutide and obesity: a review of the data so far. Drug. Des. Devel. Ther. [Internet]. 2015; 9:1867–75. Available from: http://dx.doi.org/10.2147/DDDT.S58459
8. O'Neil PM, Birkenfeld AL, McGowan B, Mosenzon O, Pedersen SD, Wharton S, et al. Efficacy and safety of semaglutide compared with liraglutide and placebo for weight loss in patients with obesity: a randomised, double-blind, placebo and active controlled, dose-ranging, phase 2 trial. Lancet [Internet]. 2018;392(10148):637–49. Available from: http://dx.doi.org/10.1016/S0140-6736(18)31773-2
9. Hasanzad M, Sarhangi N, Nikfar S, Ostad SN, Aghaei Meybodi HR. A narrative review of current trends in liraglutide: insights into the unmet needs in management of type 2 diabetes and obesity. J. Diabetes Metab. Disord. [Internet]. 2020;19(2):1863–72. Available from: http://dx.doi.org/10.1007/s40200-020-00619-9
10. Maor Y, Ergaz D, Malnick SDH, Melzer E, Neuman MG. Liraglutide-induced hepatotoxicity. Biomedicines [Internet]. 2021;9(2):106. Available from: http://dx.doi.org/10.3390/biomedicines9020106
11. Charpentier J, Briand F, Lelouvier B, Servant F, Azalbert V, Puel A, et al. Liraglutide targets the gut microbiota and the intestinal immune system to regulate insulin secretion. Acta Diabetol. [Internet]. 2021;58(7):881–97. Available from: http://dx.doi.org/10.1007/s00592-020-01657-8
12. Ma J, Hu X, Zhang W, Tao M, Wang M, Lu W. Comparison of the effects of Liraglutide, Tirzepatide, and Retatrutide on diabetic kidney disease in db/db mice. Endocrine [Internet]. 2025;87(1):159–69. Available from: http://dx.doi.org/10.1007/s12020-024-03998-8
13. Saunders KH, Shukla AP, Igel LI, Kumar RB, Aronne LJ. Pharmacotherapy for obesity. Endocrinol. Metab. Clin. North Am. [Internet]. 2016;45(3):521–38. Available from: http://dx.doi.org/10.1016/j.ecl.2016.04.005
14. Gusmão-Nascimento JW, Nunes Cruz DM, Almeida Gama L, Luz Alves WD, Machado MPR, Corá LA, et al. Liraglutide modulates morpho-functional and inflammatory gastrointestinal responses in rats. Eur. J. Clin. Invest. [Internet]. 2024;54(2):e14112. Available from: http://dx.doi.org/10.1111/eci.14112
15. Ribble D, Goldstein NB, Norris DA, Shellman YG. A simple technique for quantifying apoptosis in 96-well plates. BMC Biotechnol. [Internet]. 2005;5(1):12. Available from: http://dx.doi.org/10.1186/1472-6750-5-12
16. Pi-Sunyer X, Astrup A, Fujioka K, Greenway F, Halpern A, Krempf M, et al. A randomized, controlled trial of 3.0 mg of liraglutide in weight management. N. Engl. J. Med. [Internet]. 2015;373(1):11–22. Available from: http://dx.doi.org/10.1056/NEJMoa1411892
17. Hui H, Nourparvar A, Zhao X, Perfetti R. Glucagon-like peptide-1 inhibits apoptosis of insulin-secreting cells via a cyclic 5'-adenosine monophosphate-dependent protein kinase A- and a phosphatidylinositol 3-kinase-dependent pathway. Endocrinology [Internet]. 2003;144(4):1444–55. Available from: http://dx.doi.org/10.1210/en.2002-220897
18. Farilla L, Bulotta A, Hirshberg B, Li Calzi S, Khoury N, Noushmehr H, et al. Glucagon-like peptide 1 inhibits cell apoptosis and improves glucose responsiveness of freshly isolated human islets. Endocrinology [Internet]. 2003;144(12):5149–58. Available from: http://dx.doi.org/10.1210/en.2003-0323
19. Challa TD, Beaton N, Arnold M, Rudofsky G, Langhans W, Wolfrum C. Regulation of adipocyte formation by GLP-1/GLP-1R signaling. J. Biol. Chem. [Internet]. 2012;287(9):6421–30. Available from: http://dx.doi.org/10.1074/jbc.M111.310342
20. Quoyer J, Longuet C, Broca C, Linck N, Costes S, Varin E, et al. GLP-1 mediates antiapoptotic effect by phosphorylating Bad through a beta-arrestin 1-mediated ERK1/2 activation in pancreatic beta-cells. J. Biol. Chem. [Internet]. 2010;285(3):1989–2002. Available from: http://dx.doi.org/10.1074/jbc.M109.067207

21. Yao M, Zhang J, Li Z, Bai X, Ma J, Li Y. Liraglutide protects nucleus pulposus cells against high-glucose induced apoptosis by activating PI3K/Akt/ mTOR/caspase-3 and PI3K/Akt/GSK3β/caspase-3 signaling pathways. Front. Med. (Lausanne) [Internet]. 2021;8:630962. Available from: http://dx.doi.org/10.3389/fmed.2021.630962
22. Li Y, Hansotia T, Yusta B, Ris F, Halban PA, Drucker DJ. Glucagon-like peptide-1 receptor signaling modulates beta cell apoptosis. J. Biol. Chem. [Internet]. 2003;278(1):471–8. Available from: http://dx.doi.org/10.1074/jbc.M209423200
23. Yuhan R, Koutsouris A, Savkovic SD, Hecht G. Enteropathogenic Escherichia coli-induced myosin light chain phosphorylation alters intestinal epithelial permeability. Gastroenterology [Internet]. 1997;113(6):1873–82. Available from: http://dx.doi.org/10.1016/s0016-5085(97)70006-4
24. Fasano A, Uzzau S. Modulation of intestinal tight junctions by Zonula occludens toxin permits enteral administration of insulin and other macromolecules in an animal model. J. Clin. Investig. [Internet]. 1997; 99(6):1158–64. Available from: http://dx.doi.org/10.1172/JCI119271
25. Philpott DJ, McKay DM, Mak W, Perdue MH, Sherman PM. Signal transduction pathways involved in enterohemorrhagic Escherichia coli-induced alterations in T84 epithelial permeability. Infect. Immun.[Internet]. 1998;66(4):1680–7. Available from: http://dx.doi.org/10.1128/IAI.66.4.1680-1687.1998
26. Holmgren J, Czerkinsky C, Eriksson K, Mharandi A. Mucosal immunisation and adjuvants: a brief overview of recent advances and challenges. Vaccine [Internet]. 2003;21:S89–95. Available from: http://dx.doi.org/10.1016/s0264-410x(03)00206-8
27. Zhao F, Li J, Wang R, Xu H, Ma K, Kong X, et al. Exendin-4 promotes actin cytoskeleton rearrangement and protects cells from Nogo-A-Δ20 mediated spreading inhibition and growth cone collapse by down-regulating RhoA expression and activation via the PI3K pathway. Biomed. Pharmacother. [Internet]. 2019;109:135–43. Available from: http://dx.doi.org/10.1016/j.biopha.2018.10.008
28. Berven LA, Willard FS, Crouch MF. Role of the p70(S6K) pathway in regulating the actin cytoskeleton and cell migration. Exp. Cell Res. [Internet]. 2004;296(2):183–95. Available from: http://dx.doi.org/10.1016/j.yexcr.2003.12.032
29. Chandrasekher G, Kakazu AH, Bazan HEP. HGF- and KGF-induced activation of PI-3K/p70 S6 kinase pathway in corneal epithelial cells: Its relevance in wound healing. Exp. Eye Res. [Internet]. 2001;73(2):191–202. Available from: http://dx.doi.org/10.1006/exer.2001.1026